Performance improvement of organic solar cells with the introduction of branched zinc oxide nanorods

Fanan Wei[1,2], *Minlin Jiang*[3], *Lei Zhou*[1,2], *Zaili Dong*[1,2]

[1]*State Key Laboratory of Robotics, Shenyang Institute of Automation, Chinese Academy of Sciences, Shenyang 110016, People's Republic of China*
[2]*University of Chinese Academy of Sciences, Beijing 100049, People's Republic of China*
[3]*Department of Electrical and Computer Engineering, University of Pittsburgh, Pittsburgh 15261, USA*
E-mail: dzl@sia.cn

Published in Micro & Nano Letters; Received on 8th February 2015; Revised on 29th March 2015; Accepted on 1st April 2015

Zinc oxide (ZnO) nanorods with branches are synthesised through facile hydrothermal approach at relatively low temperature. With the prepared ZnO nanostructures as the hole-blocking layer, organic solar cells based on poly(3-hexylthiophene): 1-(3-methoxycarbonyl) propyl-1-phenyl[6,6]C61 are fabricated. For comparison, devices with planar ZnO thin film and bare ZnO nanorods are manufactured as well. *J–V* curves show that the best device performance is achieved by the branched nanorod-based solar cell. Owing to the decreased charge carrier travelling length, the nanorod-based device shows higher short circuit current (J_{sc}) than that of the device with planar ZnO layer. Moreover, the solar cell with branched nanorods shows larger open-circuit voltage (V_{oc}) than that with bare nanorods. Therefore, the performance of organic photovoltaic is enhanced with the introduction of branched ZnO nanorods. Finally, the mechanism of device performance improvement upon the introduction of branched nanorods is discussed.

1. Introduction: Organic solar cells, fabricated from semiconducting polymers and small molecules, have attracted a lot of attention from both academic and industrial fields. Owing to the merits, including exceptionally low fabrication cost, high flexibility and extremely light weight, organic photovoltaic is becoming a promising alternative to currently popular silicon-based solar cells. However, the large-scale application of the organic solar cells is still beyond practice because of the low power conversion efficiency (PCE). Even though the world record of efficiency for organic devices is more than 10% presently [1–3], a high PCE value can only be achieved at small scale and in the laboratory. Therefore, the performance of the device is still required to be enhanced greatly.

Owing to the considerably low relative dielectric permittivity (ε), of about 2–4, for most of the polymers applied in organic solar cells, the electrostatic adhesion force $F_{sat} = e^2/(4\pi\varepsilon r^2)$ between the charges with opposite sign is so high that it is impossible for the heat energy to dissociate the carrier pairs at room temperature. Then, an exciton, rather than a free electron–hole pair, is generated upon the absorption of photon in organic solar cells. The donor/acceptor (D/A) interface is the only place for exciton to be dissociated into electron and hole. In most cases, the distance from the D/A interface to the electrodes is too long for most carriers to cover; that is, plenty of the dissociated electrons and holes will meet each other and decay through recombination. The recombination between the electrons and holes contributes to a large part of the energy loss in the whole photocurrent generation process of organic solar cells.

The nanostructure, with large area to volume ratio, provides a potential solution to the problem of non-geminate recombination. Zinc oxide (ZnO), with proper energy levels, deep highest occupied molecular orbital level and large bandgap, has been widely used as the hole-blocking layer in organic devices [4]. On the other hand, various ZnO nanostructures can be prepared with facile hydrothermal solution processes. Up to now, almost all kinds of ZnO nanostructures, such as nanorods [5–9], nanotubes [10] and nanoforest [11], have been tested in dye-sensitised solar cells (DSSCs), and significant performance improvement is achieved.

On the other hand, nanostructures can help to enhance the photon absorption of solar cells through light interference because the size of the nanostructure is comparable to that of the incident light wavelength.

Herein, we attempt to use the success of ZnO nanostructures in DSSCs to promote the performance of organic solar cells. Some groups have already applied ZnO nanorods into organic solar cells [12]. However, the fundamental mechanism of the performance enhancement with ZnO nanorods is still far from clear and the device performance is expected to be improved further with branched nanorods. In this Letter, we attempted to reveal the working principle of nanorods in organic devices and try to apply branched nanorods into organic solar cells.

2. Experiments and methods

2.1. Synthesis of ZnO nanorods: The recipe for ZnO nanorods growth is similar to that from [13] with minor modification. Four pieces of glass slides (1.5 cm*2.5 cm), labelled A, B, C and D, are washed and rinsed with deionised (DI) water, isopropanol and acetone by ultrasonication for 10 min, respectively. After UV–ozone treatment of the slides for 10 min. TiO_2 sol–gel is deposited onto the glass slides to guarantee the block of holes. Then the samples are baked at 200°C for 5 min, followed by annealing at 450°C for 30 min. For the next step, the ZnO seed layer is deposited on the slides from the ethanol solution of zinc acetate. For sample A, Zn^{2+} concentration in the seed solution is 50 mM, whereas, for the others, the concentration is 5 mM. Subsequently, the slides are annealed at 150°C for 2 min and then 550°C for 30 min on a hot plate. ZnO nanorods are grown on the slides (B–D) by placing the glass slides in a nutrition solution (zinc acetate 20 mM and hexamethylenetetramine 20 mM) with top side down. The synthesis process is conducted in a hot water bath at 95°C for 2 h.

2.2. Synthesis of branched ZnO nanorods: The branched ZnO nanorod preparation recipe is similar to that in [14]. To be brief, samples C and D are immersed in a solution of 57 mM zinc acetate and 500 mM NaOH. A solution of 0.57 M zinc acetate and 5 M NaOH is prepared first and then diluted ten times. The reaction is performed at 98°C for 1 h. For sample D, 50 µl of PEI (polyethylenimine, branched ethylenediamine, Sigma-Aldrich) is added into 20 ml of reaction solution.

doi: 10.1049/mnl.2015.0052

2.3. Device fabrication: The slides with ZnO nanostructures grown are used to fabricate organic solar cells. For a planar device (A), the polymer solution concentration is 20 mg/ml for each component (poly(3-hexylthiophene) (P3HT) and 1-(3-methoxycarbonyl) propyl-1-phenyl[6,6]C61) (PCBM). The spin speed is 1000 rpm, 10 s; 2000rpm, 40 s. However, for the other samples, the concentration is set to be 2 mg/ml for each component. The solution is dropped onto the samples (0.2 ml each time, two times), followed by annealing at 120°C for 25 min and is then cooled down for 20 min before next deposition. The device fabrication process is carried out in a glove box with nitrogen protection.

The electron-blocking layer, poly (3, 4- ethylenedioxythiophene) polystyrene sulphonate (PEDOT:PSS), is spin coated on samples at a speed of 1000 rpm, 10 s for the first stage and 5000 rpm, 40 s for the second stage. The PEDOT:PSS solution is mixed with 1% Triton-X 100 before deposition. Then, the samples are baked at 120°C for 15 min.

Finally, the anode, silver layer, is evaporated onto samples through a mask using an e-beam evaporator. The thickness of the anode layer is controlled to be 90 nm. Fig. 1 takes sample C fabrication as an example to illustrate the device fabrication scheme.

2.4. Characterisation: The ZnO nanorods and branched ZnO nanorods grown on glass slides are characterised by X-ray diffraction (XRD) and scanning electron microscope (SEM).

To compare the performance of the organic solar cells fabricated with varied nanostructures, the current–voltage responses of the devices are characterised by a source meter (Keithley 2601) both in the dark and under 100 mW/cm^2 illumination. The illumination is supplied by a sunlight simulator (Newport 69907) and the power is calibrated with an optical power meter (Thorlabs GmbH PM 100).

3. Results and discussion: As indicated by the XRD patterns in Fig. 2, the synthesised ZnO nanorods show a crystalline nature. Moreover, a comparison of XRD results from both the bare and branched nanorods tells little difference between them, which indicates the nice crystalline structure of both the trunks and branches in the nanostructures.

SEM images of the ZnO nanostructures, including nanorods and branched nanorods, are displayed in Fig. 3. As demonstrated from the SEM images, branches are uniformly distributed at the wall of the nanorods. PEI prefers to cover the side wall of the ZnO nanorods, so the size of the branches in sample D is less than that in sample C, as observed in Figs. 3*c* and *d*.

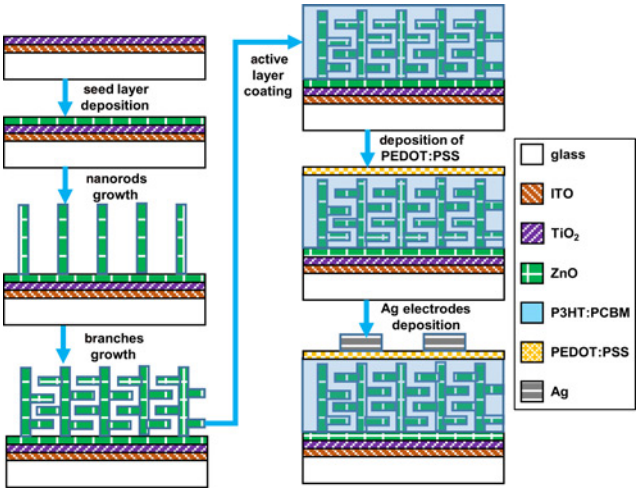

Figure 1 *Schematic of branched ZnO nanorods synthesis and subsequent organic solar cells fabrication process*

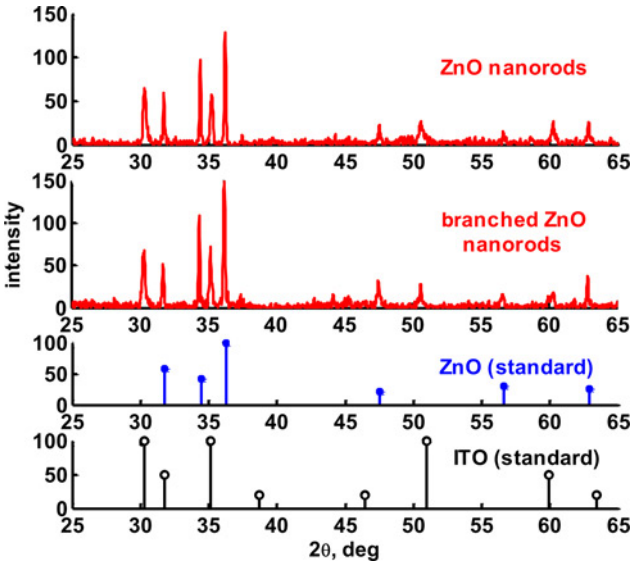

Figure 2 *XRD results of bare and branched ZnO nanorods*
Since nanorods are prepared on ITO glass, peaks contributed by ITO are observed

Fig. 4 presents the cross-sectional SEM images of the fabricated devices with ZnO nanostrucutres. The thickness of the devices is around 2 µm. The indium tin oxide (ITO) layer is measured to be around 150 nm, which agrees well with the nominal value. The active materials penetrate into the gaps between nanorods so well that the effectiveness of devices is guaranteed. For a branched

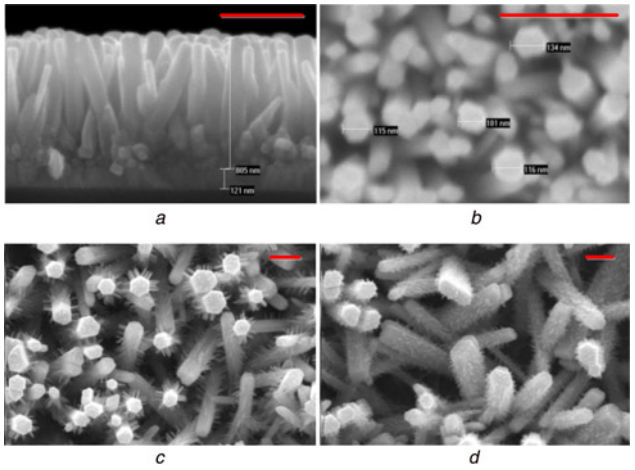

Figure 3 *SEM images of synthesised ZnO nanostructures*
a and *b* Cross section and surface SEM images of ZnO nanorods
c and *d* Surface SEM images of branched ZnO nanorods synthesised without and with PEI, respectively
Scale bar in *a* and *b* is 500 nm. Scale bar in *c* and *d* is 1 µm

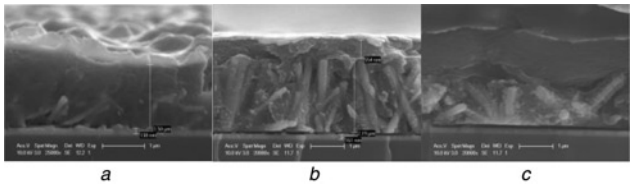

Figure 4 *SEM images of cross section of samples*
a For sample B
b For sample C
c For sample D

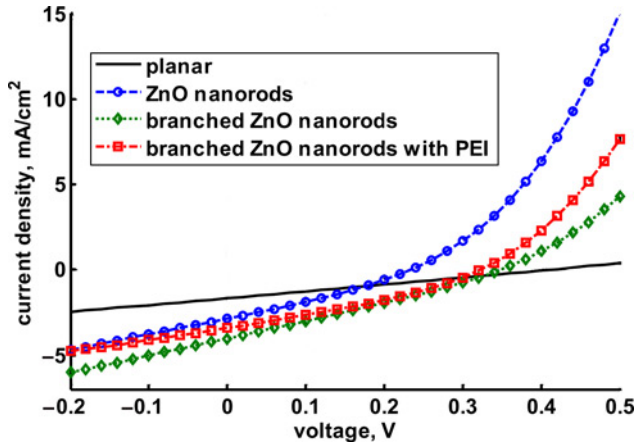

Figure 5 *J–V response of organic solar cells fabricated with different ZnO nanostructures*

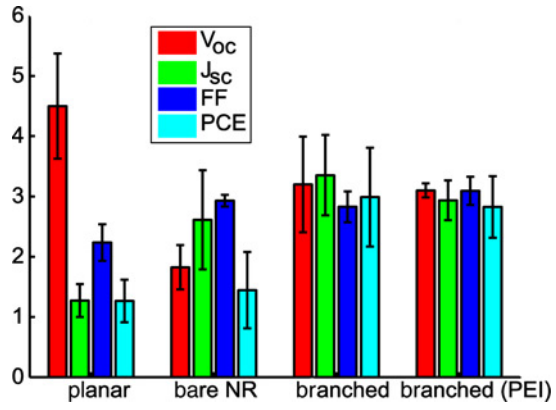

Figure 6 *Bar plot of performance indices for various organic solar cells tested*
Average values and standard deviation values for V_{oc}, J_{sc}, FF and PCE are estimated from *J–V* curves acquired from four devices for each case (for better observation, V_{oc}, FF and PCE are multiplied by 10 in the plot)

nanorods-based device, the branches are still obvious from cross-sectional SEM image of the solar cell.

J–V curves for the fabricated typical organic solar cells with different structures are obtained under the same conditions and are presented in Fig. 5.

Major performance indices of the characterised solar cells are summarised in Table 1 and Fig. 6. The data are obtained from four solar cells for each type of device structure. As indicated in Table 1, sample A (the planar device) possesses the highest V_{oc}. Compared with the bare nanorods-based device, the branched nanorods-based device achieves higher values for V_{oc}, J_{sc} and PCE. The device with bare ZnO nanorods won the champion of fill factor (FF).

To clarify the fundamental mechanism of performance index increasing with the introduction of ZnO nanorods, light distribution in the device is simulated by solving Maxwell's equations using COMSOL 4.3a. For simplification, the wavelength of the incident light is set to be 500 nm. Owing to the size effect of the nanorods, more light energy is trapped in the active layer part, as shown in Figs. 7*b* and *c*. Therefore, the charge carrier concentration upon light irradiation is projected to be higher in the ZnO nanorods-based devices than that in the planar ZnO thin film-based devices. Moreover, the branched nanorods can help to enhance light absorption even further as revealed from Fig. 7*c*. Since excitons can also be dissociated at the P3HT/ZnO interface, the carrier concentration is expected to be increased further with ZnO nanorods. Moreover, because of the larger interface area, branched nanostructures based ones will benefit even more from the P3HT/ZnO interface splitting of excitons. Therefore, J_{sc} of the nanorods-based device is higher than that of planar devices, but lower than that of branched nanorods-based devices. According to (1), higher charge carrier concentration also results in higher V_{oc}. Therefore, the branched nanorods got higher V_{oc} than bare nanorods. However, because the thickness of planar devices is relatively smaller than those

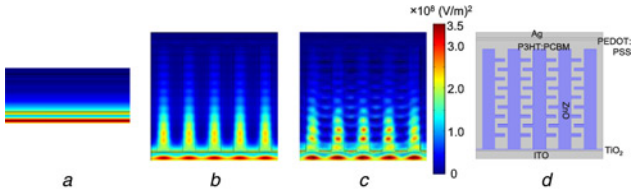

Figure 7 *Simulation results of $|E|^2$, light electric field distribution in devices with planar*
a ZnO layer
b ZnO nanorods
c Branched ZnO nanorods
Simulations are implemented using COMSOL multiphysics 4.3b (*a–c* shares the same legend)
d Illustrates device structure of branched ZnO nanorods based solar cells used in the simulation
All refractive index data of materials are acquired from [15]

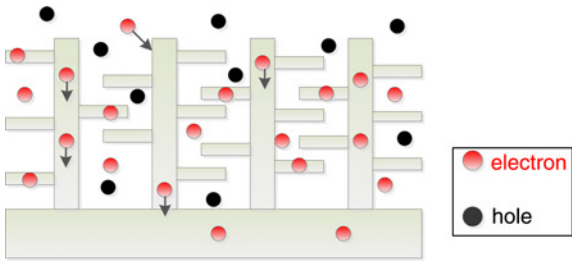

Figure 8 *Schematic of branched ZnO nanorods-based solar cells*
Electrons will be extracted towards the cathode by travelling through ZnO nanorods, while the holes are blocked

Table 1 Performance indices of devices with different ZnO structures

	A	B	C	D
V_{oc}, V	0.450 ± 0.0872	0.1825 ± 0.0369	0.320 ± 0.0794	0.310 ± 0.0115
J_{sc}, mA/cm^2	1.272 ± 0.2708	2.6117 ± 0.8228	3.353 ± 0.6665	2.9352 ± 0.3291
FF	0.2234 ± 0.0304	0.2928 ± 0.0097	0.2829 ± 0.0255	0.3093 ± 0.0234
PCE, %	0.1266 ± 0.0352	0.1445 ± 0.0633	0.2989 ± 0.0818	0.2826 ± 0.0510

A – ZnO thin film; B – nanorods; C – branched nanorods; and D – branched nanorods synthesised with PEI. The average and standard deviation values are estimated from four devices for each type of device.

doi: 10.1049/mnl.2015.0052

with bare and branched nanorods, the highest V_{oc} is achieved by planar devices; that agrees well with the reported results [16, 17].

Furthermore, with the ZnO nanorods, the generated electrons can be extracted by the neighbouring ZnO easily. The electron extraction process is largely facilitated with the introduction of nanostructures (Fig. 8). Besides, because of the n-type nature of ZnO, holes will be blocked from ZnO. Hence, the possibility of electrons and holes meeting is largely reduced, thus the non-geminate recombination can be relieved. Therefore, both nanorods and branched nanorods-based solar cells gets higher FF than that of planar device.

A comparison between samples C and D verifies that the size of ZnO branches contributes little to device performance.

4. Conclusion: Herein, we introduce branched ZnO nanorods into the organic photovoltaic and enhance the device performance considerably. The performance improvement can be ascribed to two major factors. First, with branched nanorods, light absorption is enhanced because of the light trapping effect. Higher photon absorption efficiency will lead to higher carrier concentration and subsequently higher J_{sc}. Second, because of the shorter charge carrier travelling length, non-geminate recombination can be largely enhanced. Then, FF is predicted to be improved with nanorods.

In summary, the performance of organic solar cells is significantly improved through the introduction of branched ZnO nanorods into the device. Moreover, there is still much margin for the nanostructures in the promotion of organic solar cells. For future work, we will combine the experiments with the simulation approach (as we developed in [18]) to optimise device structure and fabrication process so as to achieve higher PCE, as expected. Moreover, active layer thickness, as demonstrated from both theoretical calculation and experimental test [19, 20], plays a vital role in determining the performance of organic solar cells. In the further work, we will also fully investigate the impact of branched nanorods' length on the device performance indices.

5. Acknowledgment: This research work was supported by the National Natural Science Foundation of China (project no. 61327014).

6 References

[1] Kaneko H., Ochiai Y., Shimizu K., Hosokawa Y., Gokon N., Tamaura Y.: 'Thermodynamic study based on the phase diagram of the Na_2O-MnO-Fe_2O_3 system for H-2 production in three-step water splitting with Na_2Co_3/$MnFe_2O_4$/Fe_2O_3', *Sol. Energy*, 2002, **72**, (4), pp. 377–383

[2] You J.B., Dou L.T., Yoshimura K., *ET AL.*: 'A polymer tandem solar cell with 10.6% power conversion efficiency', *Nat. Commun.*, 2013, **4**, doi: 10.1038/ncomms2411

[3] http://www.nrel.gov/, accessed date 2014

[4] Wang J.C., Weng W.T., Tsai M.Y., *ET AL.*: 'Highly efficient flexible inverted organic solar cells using atomic layer deposited ZnO as electron selective layer', *J. Mater. Chem.*, 2010, **20**, (5), pp. 862–866

[5] Xu C.K., Shin P., Cao L.L., Gao D.: 'Preferential growth of long ZnO nanowire array and its application in dye-sensitized solar cells', *J. Phys. Chem. C*, 2010, **114**, (1), pp. 125–129

[6] Desai U.V., Xu C.K., Wu J.M., Gao D.: 'Solid-state dye-sensitized solar cells based on ordered ZnO nanowire arrays', *Nanotechnology*, 2012, **23**, (20) p. 205401

[7] Baxter J.B., Aydil E.S.: 'Nanowire-based dye-sensitized solar cells', *Appl. Phys. Lett.*, 2005, **86**, (5), pp. 053114-1–053114-3

[8] Law M., Greene L.E., Johnson J.C., Saykally R., Yang P.D.: 'Nanowire dye-sensitized solar cells', *Nat. Mater.*, 2005, **4**, (6), pp. 455–459

[9] Chen L.L., Li X.D., Qu L.L., *ET AL.*: 'Facile and fast one-pot synthesis of ultra-long porous ZnO nanowire arrays for efficient dye-sensitized solar cells', *J. Alloy Compd.*, 2014, **586**, pp. 766–772

[10] Xi Y., Wu W.Z., Fang H., Hu C.G.: 'Integrated ZnO nanotube arrays as efficient dye-sensitized solar cells', *J. Alloy Compd.*, 2012, **529**, pp. 163–168

[11] Ko S.H., Lee D., Kang H.W., *ET AL.*: 'Nanoforest of hydrothermally grown hierarchical ZnO nanowires for a high efficiency dye-sensitized solar cell', *Nano. Lett.*, 2011, **11**, (2), pp. 666–671

[12] Huang J.S., Chou C.Y., Liu M.Y., Tsai K.H., Lin W.H., Lin C.F.: 'Solution-processed vanadium oxide as an anode interlayer for inverted polymer solar cells hybridized with ZnO nanorods', *Org. Electron.*, 2009, **10**, (6), pp. 1060–1065

[13] Greene L.E., Yuhas B.D., Law M., Zitoun D., Yang P.D.: 'Solution-grown zinc oxide nanowires', *Inorg. Chem.*, 2006, **45**, (19), pp. 7535–7543

[14] Wu C.T., Liao W.P., Wu J.J.: 'Three-dimensional ZnO nanodendrite/nanoparticle composite solar cells', *J. Mater. Chem.*, 2011, **21**, (9), pp. 2871–2876

[15] Wang J., Pan S.L., Chen M.Y., Dixon D.A.: 'Gold nanorod-enhanced light absorption and photoelectrochemical performance of alpha-Fe_2O_3 thin-film electrode for solar water splitting', *J. Phys. Chem. C*, 2013, **117**, (42), pp. 22060–22068

[16] Sievers D.W., Shrotriya V., Yang Y.: 'Modeling optical effects and thickness dependent current in polymer bulk-heterojunction solar cells', *J. Appl. Phys.*, 2006, **100**, (11) p. 114509

[17] Kumar P., Kumar H., Jain S.C., Venkatesu P., Chand S., Kumar V.: 'Effect of active layer thickness on open circuit voltage in organic photovoltaic devices', *Jpn. J. Appl. Phys.*, 2009, **48**, (12), doi: 10.1143/JJAP.48.121501

[18] Wei F.N., Liu L.M., Liu L.Q., Li G.Y.: 'Multiscale modeling and simulation for optimizing polymer bulk heterojunction solar cells', *IEEE J. Photovolt.*, 2013, **3**, (1), pp. 300–309

[19] Shen H.H., Bienstman P., Maes B.: 'Plasmonic absorption enhancement in organic solar cells with thin active layers', *J. Appl. Phys.*, 2009, **106**, (7), doi: 10.1063/1.3243163

[20] He Z.C., Zhong C.M., Su S.J., Xu M., Wu H.B., Cao Y.: 'Enhanced power-conversion efficiency in polymer solar cells using an inverted device structure', *Nat. Photonics.*, 2012, **6**, (9), pp. 591–595